POLYMER REACTION ENGINEERING

Indexing and Abstracting Services. Articles published in *Polymer Reaction Engineering* are selectively indexed or abstracted in:

CEABA ■ Chemical Abstracts ■ Current Contents/Engineering, Computing, and Technology ■ Engineering Index/COMPENDEX PLUS ■ ISI Alerting Services ■ Materials Information ■ Materials Science Citation Index ■ Plastics Rubber Fibers ■ Polymer Contents ■ Rapra Abstracts Database ■ Referativnyi Zhurnal/Russian Academy of Sciences ■ Research Alert ■ Science Citation Index ■ SciSearch/SCI-Expanded

Manuscript Preparation and Submission. See end of issue.

www.dekker.com

POLYMER REACTION ENGINEERING, 9(3), 163–182 (2001)

EFFECT OF MULTIPLE FEEDINGS IN THE OPERATION OF A HIGH-PRESSURE POLYMERIZATION REACTOR FOR ETHYLENE POLYMERIZATION

M. Asteasuain, P. E. Ugrin, M. H. Lacunza, and A. Brandolin*

Planta Piloto de Ingeniería Química - UNS-CONICET
Camino La Carrindanga, km 7 - 8000 Bahía
Blanca - Argentina

ABSTRACT

A thorough model of the high pressure polymerization of ethylene in tubular reactors previously developed by the authors is used to analyze operating conditions for a specific industrial reactor. The objective is to maximize productivity while keeping product quality within desired parameters. The variables under analysis are: position, rate and temperature of lateral reactor feeds, reactor jacket configuration, temperature and flow rate of the refrigerant. Separating the initiator injections provides an increase in conversion, but also in polydispersity. However, this undesirable effect in polydispersity can be sorted out by manipulating the modifier flow rate properly. Besides, the refrigerating cost can be significantly reduced by means of a proper jacket configuration and an optimized refrigerant flow rate. In this way we show the usefulness of

* Corresponding author. Fax: (54)-2914861600; E-mail: abrandolin@plapiqui.edu.ar

the mathematical model as a predictive [illegible] in comparison with pilot or industrial scale trials- especial[illegible] hen processes are carried out under severe operating conditions.

INTRODUCTION

Polymerizations are highly complex processes, often carried out under severe operating conditions. This has stimulated an exhaustive study of the chemical reactions and physical properties involved, in order to generate mathematical models which are as precise as possible. These models make it possible to analyze the influence of different design and operative variables on production and product quality both safely and economically.

We are concerned here with ethylene polymerization in particular. Polyethylene is a material of widespread industrial applicability. It is obtained by the polymerization of ethylene monomer, following different processes from which different kinds of polymers result. Polyethylene properties depend on the operating conditions, as well as on the catalyst or initiator used. In this work we study the high-pressure ethylene polymerization in a tubular reactor which produces low-density polyethylene. The operating conditions are rather severe: pressure is between 1300 and 3000 atm, and temperature varies from 50 to 330 °C along the axial length as a result of highly exothermic reactions. Moreover, a pulse valve located at the reactor end periodically sends a pressure pulse in order to separate the polymer added to the reactor wall. This modifies the reaction extent and the thermodynamics of the mixture.

The reactor productivity and molecular properties of the product are controlled by multiple initiator injections, chain transfer agents and monomer added at different positions along the reactor. This makes it clear that a mathematical description of this process is not an easy task and it will be more accurate as the model becomes more detailed and realistic.

A search in the literature shows that there are very few works dealing with the optimization of reactors of this kind, most of which use simplified models. For example, Lee and Marano (1979) determined the jacket temperature that maximized conversion for a given molecular weight. Besides, they performed a sensitivity analysis which involved the initiator, modifier and global heat transfer coefficient. Mavridis and Kipparissides (1985) presented an optimization strategy using a theoretical model to find the best values for the operative parameters, so as to obtain the maximum conversion for a certain polyethylene molecular weight. Results from these works present the inconvenience that they were obtained using models which assume constant jacket temperature, reactor pressure and global heat transfer coefficient. Yoon and Rhee (1985) determined optimum temperature profiles that [illegible]imized conversion. Like the previously mentioned authors, they also used a [illegible]fied model without including molecular properties in the objective function.

Recently, Kiparissides *et al.* (1993) presented simulation results illustrating the effects of initiator concentration, inlet pressure and chain transfer concentration on polymer quality and reactor operation.

Brandolin et al. (1991) studied optimal policies for operating an industrial reactor, while keeping molecular properties within desired values. They used a model that considered a single oxygen initiation, constant pressure and variable jacket temperature. Afterwards, our research group (Lacunza et al., 1998a) performed a parametric analysis with the purpose of finding the optimum operating conditions that maximized conversion, while keeping the product within desired specifications as regards polydispersity and long-chain branching indexes. Monomer and initiator flows, positions and temperatures of all feeds were analyzed by means of a thorough model of the reactor (Brandolin et al., 1996).

In this paper we go further on with that kind of analysis. We have studied the influence of monomer feeding points with simultaneous initiator injection, monomer and modifier flow rates on reactor productivity and product quality. Product quality was measured in terms of molecular weight, polydispersity and long-chain branching indexes. The former model by Brandolin et al. (1996) was used to perform the analysis. The situation investigated consisted in splitting the main feed: part of it was derived into two lateral feeds, varying their position and proportion. In all cases, the lateral feeds were accompanied by an initiator injection, whose flow rate and composition were kept constant. In addition to this, the effect of varying modifier's flow rate so as to keep polydispersity in the desired value was studied. Moreover, different jacket configurations were analyzed with the purpose of reducing refrigerating costs.

MODEL DESCRIPTION

Our mathematical model for the polymerization reactor assumes plug flow and supercritical reaction mixture; besides, it considers variation of physical and transport properties along the axial length. It also includes the pressure pulse and the option to use experimental values for the global heat transfer coefficient or to calculate it either with the ad-hoc model by Lacunza et al. (1998b) or with usual correlations. A generalized kinetic mechanism for this process (Equations 1 to 12) is shown in Table 1. The basic reactions for the free radical polymerization are initiation, propagation and termination. Thermal degradation is one of the reactions that allows good prediction of temperature profiles. Transfer to polymer enables the prediction of long-chain branching and the high polydis-

Table 1. Kinetic Mechanism

Peroxide Initiation		
$I \xrightarrow{k_c} 2R_1\,(0)$	$r_i = k_c[I]$	(1)
Oxygen Initiation		
$O_2 + M \xrightarrow{k_o} 2R_1\,(0)$	$r_o = k_o[M][O_2]^{1.1}$	(2)
Monomer Thermal Initiation		
$3M \xrightarrow{k_{mi}} R_1\,(1) + R_1\,(2)$	$r_{mi} = k_{mi}[M]^3$	(3)
High Temperature Peroxide Initiation		
$O_2 + R_i\,(x) \xrightarrow{f_o k_o} PO_{2_i}\,(x)$	$r_{gpo2}\,(i,x) = f_o k_o[R_i(x)][O_2]$	(4)
High Temperature Peroxide Generation		
$PO_{2_i}\,(x) \xrightarrow{f_{po2}k_{po2}} R_i\,(x)$	$r_{po2}\,(i,x) = k_{po2}[PO_{2_i}(x)]$	(5)
Propagation		
$R_i\,(x) + M \xrightarrow{k_p} R_i\,(x+1)$	$r_{p_r}\,(i,x) = k_p[M][R_i(x)]$; $r_{p_m} = k_p[M]K_{00}(R_i(x))$	(6)
Terminal Double Bond Propagation		
$R_i\,(x) + P_j\,(y) \xrightarrow{k_{dbp}} R_{i+j}\,(x+y)$	$r_{dbp_r}\,(i,x) = k_{dbp}\,K_{00}(P_i(x))[R_i(x)]$; $r_{dbp_p}\,(i,x) = k_{dbp}\,K_{00}(R_i(x))[P_i(x)]$	(7)
Termination by Combination		
$R_i\,(x) + R_j\,(y) \xrightarrow{k_{tc}} P_{i+j-1}\,(x+y)$	$r_{tc}\,(i,x) = k_{tc}K_{00}(R_i(x))[R_i(x)]$	(8)
Thermal Degradation		
$R_i\,(x) \xrightarrow{k_{tdt}} P_i\,(x) + R_1(0)$	$r_{tdt}\,(i,x) = k_{tdt}[R_i(x)]$	(9)
Chain Transfer to Monomer		
$R_i\,(x) + \mathrm{M} \xrightarrow{k_{trm}} P_i\,(x) + R_1(1)$	$r_{trm_r}\,(i,x) = k_{trm}[M][R_i(x)]$; $r_{trm_r} = k_{trm}[M]K_{00}(R_i(x))$	(10)
Chain Transfer to Polymer		
$R_i\,(x) + P_j(y) \xrightarrow{yk_{trp}} P_i\,(x) + R_{j+1}(y)$	$r_{trp_r}(i,x) = k_{trp}K_{10}(P_i(x))[R_i(x)]$; $r_{trp_p}(i,x) = k_{trp}K_{00}(R_i(x))x[P_i(x)]$	(11)
Chain Transfer to Modifier		
$R_i\,(x) + S \xrightarrow{k_{trs}} P_i\,(x) + R_1(0)$	$r_{trs_r}\,(i,x) = k_{trs}[S][R_i(x)]$; $r_{trs_s} = k_{trs}[S]K_{00}(R_i(x))$	(12)

Table 2. Main Mass and Temperature Equations

Global Mass	$\frac{d(\rho v)}{dz} = 0$	(13)
Peroxide Initiator	$\frac{d([I_j]v)}{dz} = -r_{i_j} \quad j = 1,2\ldots$	(14)
Oxygen Initiator	$\frac{d([O_2]v)}{dz} = -r_o - K_{00}\,(r_{gpo2}(i,x))$	(15)
Monomer	$\frac{d([M]v)}{dz} = -r_o - 3r_{mi} - r_{p_m} - r_{trm_m}$	(16)
Modifier	$\frac{d([S_j]v)}{dz} = -r_{trs_s} \quad j = 1,2\ldots$	(17)
Reactor Temperature	$\rho C_p v \frac{dT}{dz} = -4U(T - T_j) + r_{p_m}(-\Delta H)$	(18)
Jacket Temperature	$\frac{dT_j}{dz} = \pm i_f \frac{\pi 4U(T - T_j)}{\rho_j C_{pj} G_j} + (1 - i_f)\frac{(T_j + 290.23)^2}{5075.92 P_j}\frac{dP_j}{dz}$	(19)
Friction Pressure Drop	$\frac{dP_f}{dz} = -\rho\left(v\frac{dv}{dz} + \frac{2f_f v^2}{D}\right)$	(20)
Reactor Pressure	$P = P_f - \Delta P_{pv} e^{-\beta(t - t_p)}$	(21)

persities found in this type of reactor. For the process and operating conditions considered in this work, transfer to monomer, thermal initiation and double bond end propagation do not affect predicted temperature profiles and product properties significantly.

The main model balances (Equations 13 to 28) are listed in Tables 2 and 3. This model allows a realistic configuration of the reactor, as exemplified in Figure 1 -i.e. multiple initiator injections, co- or counter current jacket flow, lateral monomer feeds, periodic pressure pulse and the possibility for the jacket flow of a given jacket zone to come either from a water tank or from another jacket zone. Further details on the model as well as on the kinetic information may be found in Brandolin et al. (1996).

The model gives the following results: monomer conversion; reaction mixture and jacket fluid temperatures and pressures; mass fractions of oxygen, peroxides, monomer, radicals and polymer, as well as the three first moments of the chain length distribution of radicals and polymer; Peclet, Nusselt, Reynolds and Prandtl numbers; global heat transfer coefficient; velocity, density, viscosity and specific heat; average molecular weights, molecular-weight distributions and long and short branches indexes.

Table 3. Moment Equations and Molecular Properties

m^{th}, n^{th} Moment of a generic function $f_i(x)$

$$K_{mn}(f_i(x)) = \sum_{i=1}^{\infty} i^m \int_0^{\infty} x^n f_i(x)dx \tag{22}$$

m^{th}, n^{th} Moments of High Temperature Peroxide Concentration

$$\frac{d(K_{mn}(PO_{2_i}(x))v)}{dz} = K_{mn}(r_{gpo2}(i,x)) - f_{po2} K_{mn}(r_{po2}(i,x)) \tag{23}$$

m^{th}, n^{th} Moments of Radical Concentration

$$\begin{aligned}\frac{d(K_{mn}(R_i(x))v)}{dz} &= \sum_{i=1}^{Nin} 2f_j r_{i_j}\delta_{n0} + 2r_o\delta_{n0} + f_{po2} K_{00}(r_{po2}(i,x)) \\ &- K_{mn}(r_{rpo2_r}(i,x)) + (1+2^n) f_{mi} r_{mi} + nK_{mn-1}(r_{p_r}(i,x)) - K_{mn}(r_{tc}(i,x)) \\ &- K_{mn}(r_{tdi}(i,x)) + K_{00}(r_{tdi}(i,x))\delta_{n0} - K_{mn}(r_{pd}(i,x)) \\ &+ \sum_{l=0}^{m}\binom{m}{l}\sum_{p=0}^{n}\binom{n}{p} K_{lp}(r_{pd_r}(i,x)) - K_{mn}(r_{trm_r}(i,x)) - \sum_{i=1}^{Ns} K_{mn}(r_{trs_r}(i,x)) \\ &+ \sum_{i=1}^{Ns} K_{00}(r_{trs_r}(i,x))\delta_{n0} - K_{mn}(r_{trp_r}(i,x)) + \sum_{j=0}^{m}\binom{m}{n} K_{jn+1}(r_{trp_p}(i,x))\end{aligned} \tag{24}$$

m^{th}, n^{th} Moments of Polymer Concentration

$$\begin{aligned}\frac{d(K_{mn}(P_i(x))v)}{dz} &= 1/2\sum_{l=0}^{m}\binom{m}{l}\sum_{r=0}^{l}\binom{l}{r}\sum_{p=0}^{n}\binom{n}{p}(-1)^{l-r}K_{lp}(r_{tc}(i,x)) + K_{mn}(r_{tdi}(i,x)) \\ &- K_{mn}(r_{dbp_p}(i,x)) + K_{mn}(r_{trm_r}(i,x)) - \sum_{i=1}^{Ns} K_{mn}(r_{trs_r}(i,x)) \\ &- K_{mn}(r_{trp_r}(i,x)) - K_{mn+1}(r_{trp_p}(i,x))\end{aligned} \tag{25}$$

Number-Average Molecular Weight

$$Mn = 28\frac{K_{01}(P_i(x)) + K_{01}(r_i(x))}{K_{00}(P_i(x)) + K_{00}(R_i(x))} \tag{26}$$

Weight-Average Molecular Weight

$$Mw = 28\frac{K_{02}(P_i(x)) + K_{02}(R_i(x))}{K_{01}(P_i(x)) + K_{01}(R_i(x))} \tag{27}$$

Number-average Long Chain Branching

$$Lbn = \left.\frac{K_{10}(P_i(x)) + K_{10}(R_i(x))}{K_{00}(P_i(x)) + K_{00}(R_i(x))}\right| Mn \tag{28}$$

$$C = \sum_{i=1}^{Nzones} [5932 + 10.4(T_{jo,i} - 100)] W_{j,i} + 11.26\Delta P_{j,i} \tag{29}$$

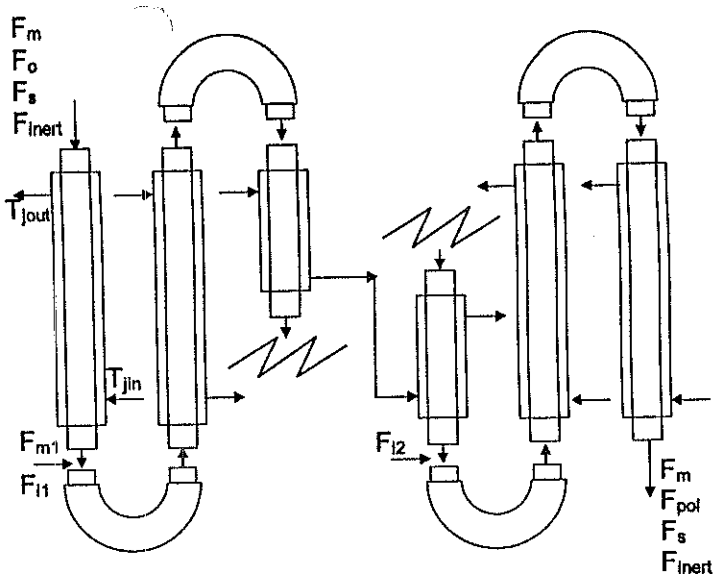

Figure 1. Reactor scheme.

PARAMETRIC ANALYSIS POLICIES

In brief the reactor under analysis has a main feed, through which the monomer, modifier and oxygen enter. In addition, there are two lateral injections of peroxide mixtures. Heating and/or cooling is achieved by means of eight jacket zones, which are independent from each other. The jacket fluids are water vapor in the first zone and liquid water in the other ones. A sensible examination of design and operative variables was performed aiming at maximizing conversion, while taking into account the molecular properties. The following subsections contain a description of this analysis.

Monomer Feed Splitting and Variation of Lateral Feeding Points

We investigated the effect of dividing the global monomer feed into a main stream introduced at the reactor entrance, and two lateral ones. The latter were always accompanied by an injection of initiator mixture, whose flow rate and composition remained constant. For each feed, different ratios R were selected with respect to the global feed (R = % main feed- % first lateral feed - % second lateral feed). Their specific values were: R = 90-10-0, 90-5-5, 90-0-10, 80-15-5, 80-10-10, 80-5-15, 70-25-5, 70-15-15, 70-5-25, 60-30-10, 60-20-20 and 60-10-30. In

lateral feed positions resulted from the combination of the following locations Nt1 and Nt2 for the first and second lateral monomer feeds respectively: Nt1: {0.031, 0.05, 0.063, 0.075, 0.094, 0.011} and Nt2: {0.375, 0.406, 0.438, 0.469, 0.500, 0.531, 0.563, 0.594, 0.625}, where Nt1 and Nt2 are relative to the total reactor length.

Modifier Flow Rate

In order to learn how the modifier flow rate influences reactor productivity and molecular properties, the modifier flow rate was changed within a range from 0.1 to 5.7 times the base case value. Conversion, number average molecular weight and polydispersity were analyzed. The objective was to be able to get a given polydispersity by manipulating the modifier flow rate.

Lateral Feed Temperatures

In all cases mentioned above, the temperature of the lateral feeds was equal to the one of the main feed. As this might be an important factor, we selected the feeding points that gave maximum conversion for each monomer split, setting feed temperatures similar to those of the reacting mixture at each position. The changes in conversion, polydispersity and average molecular weights were analyzed under those conditions.

Jacket Configuration

The jacket fluid configuration was studied with the purpose of reducing the refrigerating/heating costs, while keeping the already obtained conversion and polydispersity. We manipulated the jacket fluid flow rate and the connections between the different jacket zones. All the options were evaluated by means of Equation (29), which gives the refrigerating/heating costs (C, $/year) as a function of the jacket fluid outlet temperature ($T_{jo,i}$, °C) flow rate ($W_{j,i}$, m^3/h) and pressure drop ($\Delta P_{j,i}$, kg/cm^2). This equation takes into account the costs of treated water, pumping, purge and reposition of water evaporated in the cooling tower.

RESULTS AND DISCUSSION

The reactor under analysis has a length to diameter ratio of 27800. The base point at which this reactor operated is listed in Table 4. Figure 2 shows the final conversion as a function of the position of the lateral feeds, for three of the monomer feed distributions presented as examples.

Table 4. Base Case Operating Conditions

Component	Nt	Mass Fraction
Monomer	$6.25\ 10^{-3}$	0.987
Oxygen	$6.25\ 10^{-3}$	6.13×10^{-6}
Peroxide A	0.10	0.42
Peroxide B	0.10	0.26
Peroxide C	0.53	0.37
Peroxide D	0.10	0.14
	0.53	0.48
Peroxide E	0.10	0.19
Peroxide F	0.53	0.15
Modifier A	$6.25\ 10^{-3}$	0.0026
Modifier B	$6.25\ 10^{-3}$	0.0040
Modifier C	$6.25\ 10^{-3}$	1.46×10^{-4}
		Mass flow rate
Reacting Mixture	$6.25\ 10^{-3}$	11 kg/s
Cooling Water*	0.04, 0.21, 0.34, 0.42, 0.50, 0.59, 0.71, 0.84	1.00, 0.45, 0.37, 0.33, 0.39, 0.39 ,0.34, 0.32
	Pressures	
Inlet pressure	$6.25\ 10^{-3}$	2.32×10^8 Pa
P_{pv}	0.84	2.53×10^7 Pa
t_p	—	25 s
t_r	—	11 s
Jacket pressure	0,21, 0.34, 0.42, 0.50, 0.59, 0.71, 0.84	5.20, 2.11, 3.17, 2.11, 2.11, 3.11, 3.17
	Temperatures	
Inlet Temperature	6.25 10-3	347 K
Vapor Temperature	0.04	434 K
Water Temperature*	0.21, 0.34, 0.42, 0.50, 0.59, 0.71, 0.84	1.34, 0.97, 1.02, 0.97, 0.97, 1.01, 1.01

* Water parameters' values are reported relative to those of the vapor in the first zone.

It was observed that, for constant values of Nt2, there is a coincidence in the location of a point of maximum conversion, which in most cases corresponds to Nt1 = 0.05. In the same way there is a point of maximum conversion around Nt2 = 0.594 for constant values of Nt1. An optimum temperature for initiator injections is achieved in those positions. However, in some cases departures from this behavior were observed. This occurred when the ratio of the second monomer feed was greater than 15%. When this was the case, the previous tendency was fol-

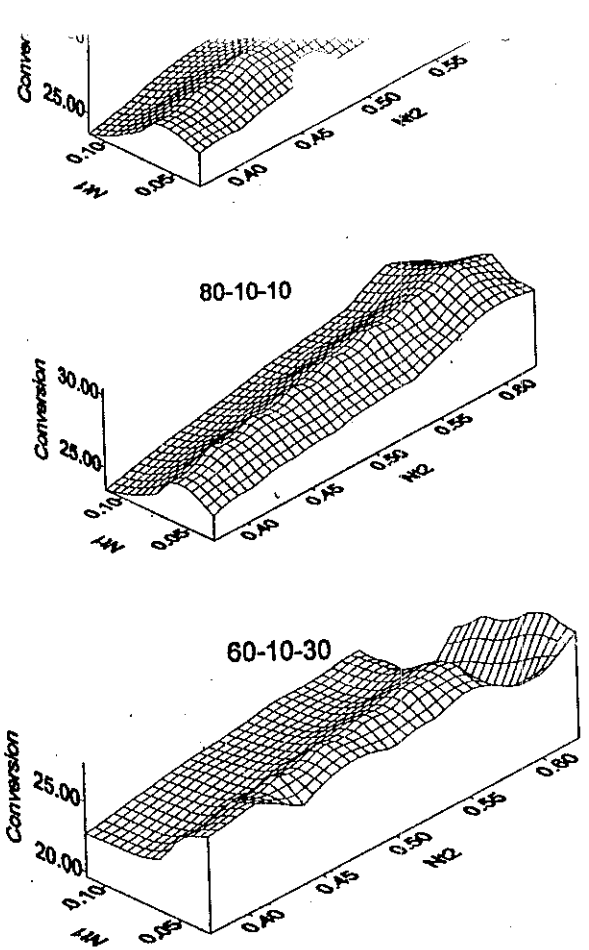

Figure 2. Conversion vs. lateral feed positions for R = 90-5-5, R = 80-10-10, and R = 60-10-30.

lowed until the position of the last monomer feed approached the reactor end. Afterwards, the conversion fell down abruptly, later rising when the second monomer feed was right at the reactor exit.

Table 5 lists the combinations of lateral monomer feed positions that gave maximum conversion. The greatest maximum conversion value corresponds to the split R = 90-10-0, which is the lowest deviation (split) of monomer along the

results can reasonably infer that the initiator feeding points rather than the monomer feed split, can increase conversion. In turn, the conversion goes down when the monomer feed split increases.

Polydispersity appears to be dependent on the position of the first monomer feed, but not on the second one, as shown in Figure 3. This remark is almost exact when the second monomer feed is small, but presents a distortion when it becomes large. In the latter, the preceding tendency is followed until the position of the second feed reaches the reactor end, bearing a close resemblance to conversion behavior. Anyway, in all cases it was observed that polydispersity decreased as the first monomer feed left the reactor entrance.

Figure 4 shows the maximum conversions and the corresponding polydispersities for each monomer feed split. In all cases, the maximum conversion was larger than the base case value. Polydispersity was around 10.5 when the maximum conversion was achieved. This value was far from the base case value of about 8, that we wanted to maintain. However, the desired value of polydispersity

Table 5. Maximum Conversion vs. Lateral Monomer Feeding Positions

R % Main, % Lateral 1, % Lateral 2	Nt1	Nt2	Conversion %
100-0-0 (base case)	0.10*	0.53*	27.22
90-10-0	0.0625	0.625	31.34
90-5-5	0.05	0.594	30.94
90-0-10	0.0625	0.954	30.67
80-15-5	0.05	0.594	30.64
80-10-10	0.05	0.594	30.55
80-5-15	0.063	0.594	30.07
70-25-5	0.050	0.594	30.38
70-15-15	0.050	0.594	29.80
70-5-25	0.0625	0.625	28.12
60-30-10	0.050	0.594	30.54
60-20-20	0.031	0.594	29.54
60-10-30	0.063	0.531	27.80

* It corresponds to initiator injection only.

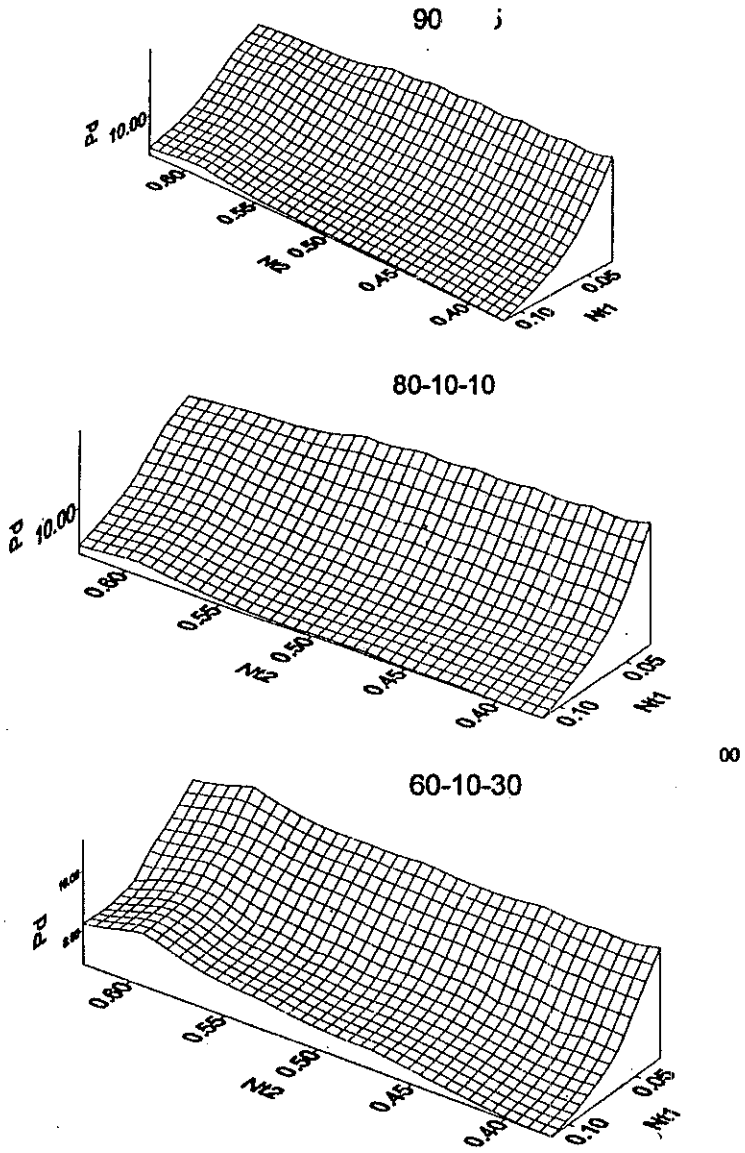

Figure 3. Polydispersity vs. lateral feed positions for R = 90-5-5, R = 80-10-10, and R = 60-10-30.

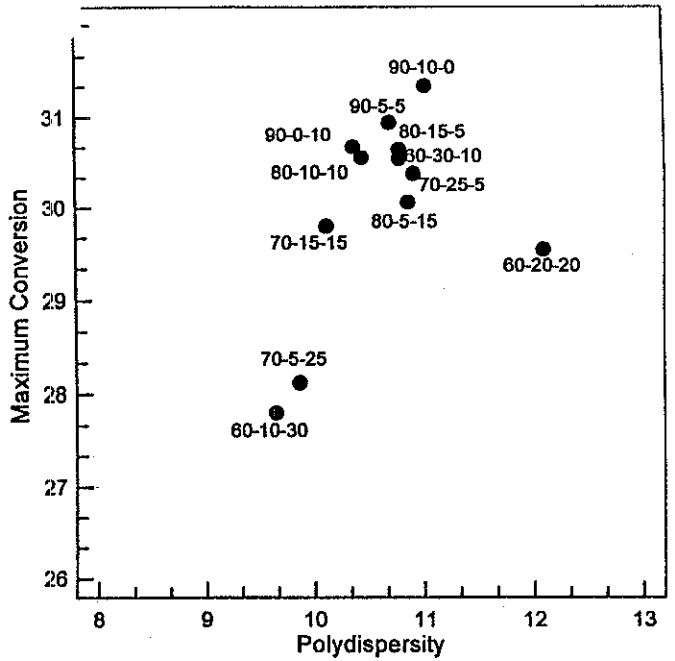

Figure 4. Maximum conversion vs. the corresponding polydispersities obtained for each monomer split.

could be achieved without great losses in conversion by manipulating the modifier flow rate, as it will be shown later. Table 6 shows molecular properties for maximum conversion for two monomer splits. Number average molecular weight, long and short branches were not significantly affected by monomer flow deviation.

Polydispersity can be adjusted at the desirable value by increasing the modifier flow rate. Figure 5 displays the dependence of number-average molecular

Table 6. Molecular Properties at Maximum Conversion. [Nt2 = 95 and Nt1 = 10 (R = 90, 5, 5)] [Nt2 = 85 and Nt1 = 10 (R= 80,15,5)]

Property	Base Case	Nt2/Nt1 = 9.5	Nt2/Nt1 = 8.5
Conversion	27.22	30.94	30.64
Mn_{calc}/Mn_{exp}	0.96	1.06	1.00
Polydispersity	7.48	10.7	10.5
LCB_{calc}/LBC_{exp} (/1000C)	0.99	1.16	1.10
SCB_{calc}/SCB_{exp} (/1000C)	0.94	0.86	0.86

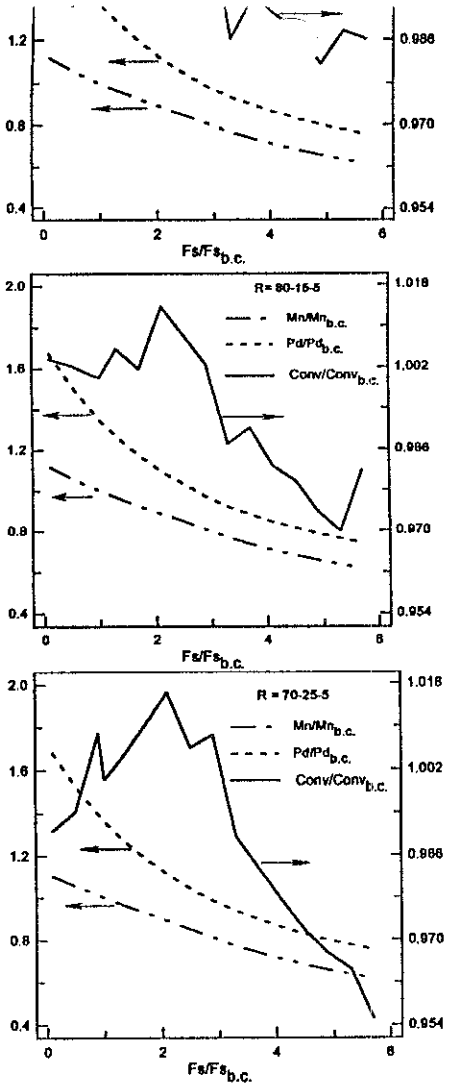

Figure 5. Number average molecular weight, polydispersity and conversion vs. modifier flow rate, for R = 90-5-5, R = 80-10-10, and R = 60-10-30. Modifier flow rate, conversion and Mn are shown relative to its corresponding base-case values; Pd is shown relative to the base-case value.

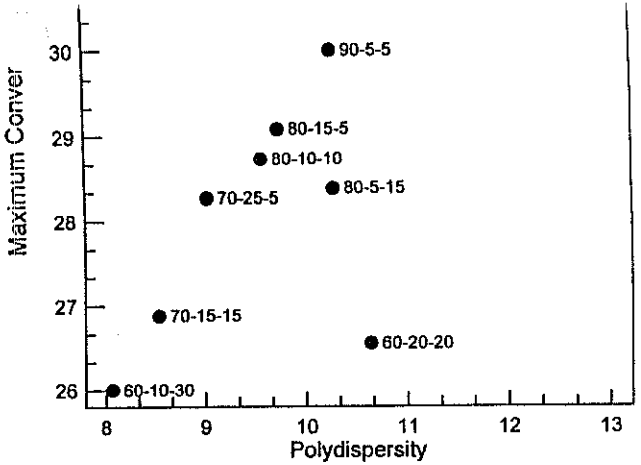

Figure 6. Maximum conversion vs. the corresponding polydispersities obtained with "hot" lateral feeds for each monomer split.

weight Mn, conversion and polydispersity Pd on modifier flow rate, for three different values of R. The corresponding lateral feed positions are those reported in Table 5. The reactor model predicted that Mn and Pd would diminish as the modifier flow rate increases, while conversion had little variation. The result was that it is necessary to increase the modifier flow rate by about two or three times in order to attain a Pd of 8, while Mn is reduced by 20%.

It was also found that when the lateral feed's temperature is set equal to that of the reaction mixture, conversion and polydispersity go down. Figure 6 presents these results for the cases that had yielded maximum conversion. This is in good agreement with previously reported results (Lacunza et al., 1998a).

Finally, the jacket fluid configuration was studied with the objective of reducing the refrigerating/heating costs. In the best result we reached, zones 5 to 8 were interconnected so that they became a single zone with counter current flow. In addition to this, the flow rates were reduced in the mentioned zones as well as

Table 7. Optimized Jacket Flows

Zone	1	2	3	4	5–8
Flow/Base Flow	0.18	0.22	1	1	0.049

Figure 7. Original (continuous line) and modified ed line) reactor jacket configurations.

in zones 1 and 2 (see Table 7). This configuration reduced the refrigerating/heating cost by 70%. Figure 7 shows a scheme of the original (continuous line) and the modified (dashed line) jacket configurations.

CONCLUSIONS

The usefulness of a comprehensive steady-state mathematical model for the high-pressure polymerization of ethylene in tubular reactors was demonstrated by determining the optimal operating conditions of an industrial reactor in order to obtain a product with predetermined properties at maximum productivity. We could find combinations of joint monomer and initiator feeding, at different monomer flow rates and feeding positions, that maximize productivity while keeping the molecular properties of the product between limits. From the results presented above, it appears that the initiator injection points rather than the split of the monomer feed are responsible for increasing conversions. We have shown that separating the injection points provides an increase both in conversion and polydispersity. The latter appears to depend mostly on the first monomer lateral feeding. The modifier flow rate proved to be a suitable control variable to keep the polydispersity within the desired value. It was also shown that it is possible to reduce refrigerating costs significantly by integrating some of the jacket zones and reducing jacket flow rates. Finally, it is not recommendable to heat the lateral feed since these results revealed that conversion and polydispersity go down.

NOMENCLATURE

Conv	Monomer conversion
C	Cost function
C_p	Heat capacity of reacting mixture
C_{pj}	Heat capacity of jacket fluid
D	Reactor internal diameter
f_f	Friction factor
f_j	Initiation efficiency of initiator "j", j = 1,2
F_{ij}	Initiator lateral flow rate "j", j = 1,2
F_{inert}	Inert flow rate
F_m	Monomer flow rate
F_o	Oxygen flow rate
F_{pol}	Polymer flow rate
f_{po2}	Efficiency of high temperature peroxide initiation
F_s	Modifier flow rate
G_j	Jacket fluid mass flow rate
I	Initiator
i_f	Jacket flow index (1: liquid, 0: vapor)
k_c	Kinetic constant for initiator decomposition
k_{dbp}	Kinetic constant for terminal double bond propagation
k_{ml}	Kinetic constant for monomer thermal initiation
k_o	Kinetic constant for oxygen decomposition
$K_{mn}(f_i(x))$	m^{th}-n^{th} order moment for the generic function $f_i(x)$, m = 0,1 . .; n = 0,1,2, . .
k_p	Kinetic constant for the propagation reaction
k_{po2}	Kinetic constant for high temperature initiator decomposition
k_{tc}	Kinetic constant for termination by combination
k_{tdt}	Kinetic constant for thermal degradation
k_{trm}	Kinetic constant for transfer to monomer reaction
k_{trp}	Kinetic constant for transfer to polymer reaction
k_{trs}	Kinetic constant for transfer to modifier reaction
Lbn	Number-average long chain branching
LCB/1000C	Long chain branching every 1000 C
M	Monomer
Mn	Number-average molecular weight
Mw	Weight-average molecular weight
N_{in}	Total number of initiators
N_s	Total number of modifiers
Nt	Relative location with respect to the total length
Ntj	Relative location of lateral monomer feed "j" or initiator injection "j", j = 1,2
Nzones	Total number of jacket zones
P	Pressure of reacting mixture
Pd	Polydispersity
P_f	Pressure due to friction effects
$P_i(x)$	Polymer molecule with "i" long-chain branches and "x" monomer units
P_j	Pressure of jacket fluid
$PO_{2i}(x)$	High temperature peroxide molecule with "i" long chain branches and "x" monomer units

R	% main feed-% first lateral [illegible] % second lateral feed
r_{dbp_r} (i,x)	Rate of radical $R_i(x)$ consum[illegible] in double bond propagation
r_{dbp_p} (i,x)	Rate of polymer $P_i(x)$ consumption in double bond propagation
r_{gpo2}(i,x)	Rate of high temperature initiator $PO_{2i}(x)$ generation
r_{po2}(i,x)	Rate of high temperature initiator $PO_{2i}(x)$ decomposition
r_i	Rate of initiator decomposition
$R_i(x)$	Radical molecule with "i" long chain branches and "x" monomer units
r_{mi}	Rate of monomer thermal initiation
r_o	Rate of oxygen initiation
r_{p_m}	Rate of monomer consumption in propagation reaction
r_{p_r}(i,x)	Rate of radical $R_i(x)$ consumption in propagation reaction
r_{tc}(i,x)	Rate of radical $R_i(x)$ consumption in termination by combination
r_{tdt}(i,x)	Rate of radical $R_i(x)$ consumption in thermal degradation
r_{trm_m}	Rate of monomer consumption in transfer to monomer reaction
r_{trm_r}(i,x)	Rate of radical $R_i(x)$ consumption in transfer to monomer reaction
r_{trp_p}(i,x)	Rate of polymer $P_i(x)$ consumption in transfer to polymer reaction
r_{trp_r}(i,x)	Rate of radical $R_i(x)$ consumption in transfer to polymer reaction
r_{trs_r}(i,x)	Rate of radical $R_i(x)$ consumption in transfer to modifier reaction
r_{trs_s}	Rate of modifier consumption in transfer to modifier reaction
S	Chain transfer agent (modifier)
SCB/1000C	Short chain branching every 1000 C
T	Temperature of the reacting mixture
t	Elapsed time after the last pulse
T_j	Jacket temperature
$T_{jo,i}$	Jacket fluid outlet temperature
t_p	Time between pulses
t_r	Recovery time between pulses
U	Global heat transfer coefficient
V	Axial velocity of reacting mixture
$W_{j,i}$	Jacket fluid volumetric flow rate
Z	Axial length

Greek Symbols

β	Adjustable coefficient in pressure pulse empirical correlation
δ_{n0}	Kronecker delta
(-ΔH)	Heat of polymerization
$\Delta P_{j,i}$	Pressure drop due to pulse valve
ΔP_{pv}	Pressure drop due to pulse valve
ρ	Density of reacting mixture
ρ_j	Density of jacket fluid

Subscripts

b.c.	Base case
calc	Calculated
exp	Experimental
in	In
out	Out
pv	Pulse valve

ACKNOWLEDGMENTS

The authors gratefully acknowledge the financial support given by CONICET (the Argentinian National Research Council) and UNS (the National University of the South).

REFERENCES

Brandolin, A., E.M. Vallés and J.N. Farber (1991). High Pressure Tubular Reactors for Ethylene Polymerization. Optimization Aspects. Polym. Eng. Sci., *31*, 381–390.

Brandolin, A., M.H. Lacunza, P.E. Ugrin and N.J. Capiati (1996). High Pressure Polymerization of Ethylene. An Improved Mathematical Model for Industrial Tubular Reactors. Polym. React. Eng. J., *4*, 193–241.

Kiparissides, C., G. Verros, G. Kalfas, M. Koutoudi and C. Kantzia (1993). A Comprehensive Mathematical Model for a Multizone Tubular High-Pressure LDPE Reactor. Chem. Eng. Comm., *121*, 193–217.

Lacunza, M.H., P.E. Ugrin and A. Brandolin (1998a). High-Pressure Polymerization of Ethylene in Tubular Reactors. A Parametric Study to Obtain Maximum Productivity. Lat. Amer. Appl. Res., *28*, 101–107.

Lacunza, M.H., P.E. Ugrin, A. Brandolin and N.J. Capiati (1998b). Heat Transfer Coefficient in a High Pressure Tubular Reactor for Ethylene Polymerization. Polym. Eng. Sci., *38*, 992–1013.

Lee K.H. and J.P. Marano, Jr. (1979). Free-Radical Polymerization: Sensitivity of Conversion and Molecular Weights to Reactor Conditions. In Polymerization Reactors and Processes, J.N. Henderson and T.C. Bouton (Eds.) ACS

Symposium. Series 104, American Che l Society: Washington D.C., 221–251.
Mavridis H. and C. Kiparissides (1985). Optimization of a High-Pressure Polyethylene Reactor, Polym. Proc. Eng., *3*, 263–290.
Yoon, B.J. and H.K. Rhee (1985). A Study of the High-Pressure Polyethylene Tubular Reactor. Chem. Eng. Commun., *34*, 253–265.

Received August 17, 2000
Accepted January 3, 2001

EMULSION/MINIEMULSION POLYMERIZATION OF BUTYL ACRYLATE WITH THE CUMENE HYDROPEROXIDE/TETRAETHLENEPENTAMINE REDOX INITIATOR

Yingwu Luo,[1] F. Joseph Schork,[1,*] Yulin Deng,[2] and Zegui Yan[2]

[1]School of Chemical Engineering, Georgia Institute of Technology, Atlanta, Georgia 30332-0100, USA
[2]Institute of Paper Science and Technology, 500 10th Street, NW, Atlanta, Georgia 30318-5794, USA

ABSTRACT

The macro- and miniemulsion polymerization of butyl acrylate (BA) with cumene hydroperoxide/tetraethlenepentamine (CHP/-TEPA) as a redox initiator system was investigated. It was found that the rate of polymerization was monotonically decreasing rather than going through a maximum as is common in emulsion polymerization. Furthermore, the polymerization rate at high monomer conversion of macroemulsion polymerization was unexpectedly decreased with an increase in initiator concentration. For miniemulsion polymerization, the polymerization stopped at rather low conversion. It was also found that the average number of free radicals per particle dropped very quickly with polymerization

* Corresponding author.